PROCEEDINGS OF SCIENCE

Astrophysical interpretation of energy spectrum and mass composition of cosmic rays as measured at the Pierre Auger Observatory

PoS(TAUP2023)125

Eleonora Guido[a,*] **on behalf of the Pierre Auger Collaboration**[b]

[a] *Experimentelle Astroteilchenphysik, Center for Particle Physics Siegen, Universität Siegen, Germany*
[b] *Observatorio Pierre Auger, Av. San Martín Norte 304, 5613 Malargüe, Argentina*
Full author list: *https://www.auger.org/archive/authors_2023_11.html*

E-mail: spokespersons@auger.org

The combined interpretation of the spectrum and composition measurements plays a key role in the quest for the origin of ultra-high-energy cosmic rays (UHECRs). The Pierre Auger Observatory, thanks to its huge exposure, provides the most precise measurement of the energy spectrum of UHECRs and the most reliable information on their composition, exploiting the distributions of the depth of maximum of the showers in the atmosphere. A combined fit of a simple astrophysical model of UHECR sources to the spectrum and mass composition measurements is used to evaluate the constraining power of the data measured by the Pierre Auger Observatory on the source properties. We find that our data across the "ankle" feature are well reproduced if two extragalactic populations of sources are considered, one emitting a very soft spectrum which dominates the region below the ankle, and the other taking over at energies above the ankle, with an intermediate mixed composition, a hard spectrum and a low rigidity cutoff. Interestingly, similar results can also be obtained if the medium-mass contribution at lower energy is provided by an additional galactic component.

XVIII International Conference on Topics in Astroparticle and Underground Physics (TAUP2023)
28.08_01.09.2023
University of Vienna

*Speaker

1. Introduction

The Pierre Auger Observatory has been providing high-quality data offering insights into the origin and nature of ultra-high-energy cosmic rays (UHECR). The spectrum exhibits distinct features, including the "ankle" at $\sim 10^{18.7}$ eV, the "instep" at $\sim 10^{19.1}$ eV, and a flux suppression above $\sim 10^{19.7}$ eV. On the other hand, the mass composition of UHECRs evolves from light elements below the ankle to increasingly heavier elements above it. Investigating the origin of UHECRs is crucial, especially in the energy range between the second knee and the ankle, where the transition from galactic to extragalactic sources occurs. This analysis aims to constrain the physical parameters governing UHECR energy spectrum and mass composition, by fitting a model involving extragalactic sources and potential galactic contributions to the data above $10^{17.8}$ eV. Further details can be found in Ref. [1].

The astrophysical model used in this analysis considers two extragalactic components, either originating from distinct populations of sources or from the interactions of nuclei in the source environment of the same population. The sources are uniformly distributed in the comoving volume, with a local overdensity within 30 Mpc to account for the Milky Way's location in a galaxy group. Each extragalactic source population's particle spectrum comprises contributions from up to five representative nuclear species, following a power-law spectrum with a rigidity-dependent broken exponential cutoff. The generation rate $\widetilde{Q}_A(E)$ for each species A is defined by a set of parameters, including the spectral index γ, the rigidity cutoff R_{cut}, and partial normalizations $\widetilde{Q}_{0A}$. Mass fractions are expressed in terms of I_A, the source emissivity of each species at redshift $z = 0$. The possible presence of a galactic component at Earth is also considered and modeled as a power law with $\gamma_{\text{Gal}} \sim 3$ and an exponential cutoff. The modification of the extragalactic fluxes due to adiabatic energy losses and interactions with background photons (CMB and EBL) occurring during the propagation is considered through SimProp simulations [2]. Finally, the mass composition is determined by using $X_{\max}$ distributions as an estimator and is subjected to the choice of hadronic interaction model (Epos-LHC [3] or Sibyll 2.3d [4]).

2. Combined fit across the ankle

The energy spectrum data is binned in logarithmic bins of width 0.1 decades from $10^{17.8}$ eV to $10^{20.2}$ eV, while the $X_{\max}$ distributions are binned from $10^{17.8}$ eV to $10^{19.6}$ eV with one additional bin for higher-energy events. The fit minimizes a deviance function D consisting of two terms, D_J for the energy spectrum and $D_{X_{\max}}$ for $X_{\max}$ distributions, using a generalized χ^2 approach. The best-fit parameters are obtained by minimizing D, and uncertainties are determined using the Minuit package and Monte Carlo simulations.

Two reference scenarios are considered. In "Scenario 1", an extragalactic component with mixed mass composition dominates at high energies, while an additional extragalactic population of pure protons dominates at low energies, where a heavier galactic contribution coexists. In "Scenario 2", the ankle feature is attributed to the superposition of two mixed extragalactic components with different spectral parameters. Both scenarios require hard spectra for the high-energy (HE) component and steep spectra for the low-energy (LE) component, as shown in the left panel of Fig. 1, as an example. In particular, the LE component is so steep that it is rapidly suppressed even in absence of an exponential cutoff, making the fit degenerate with respect to the R_{cut} value if $\gg 10^{19.5}$ V and insensitive to the details of the cutoff shape. The two extragalactic components, in presence or not of a secondary galactic contribution, reasonably succeed to reproduce the ankle feature, whose sharpness would be hardly described by other scenarios. As concerns the instep at $\sim 10^{19}$ eV, it is here given by the interplay of light-to-intermediate nuclei, as shown in the right panel of Fig. 1. Finally, the rigidity cutoff resulting from the fit suggests that the maximum energy emitted at the sources of the HE population is not high enough to entirely attribute the suppression at the highest energies to propagation effects.

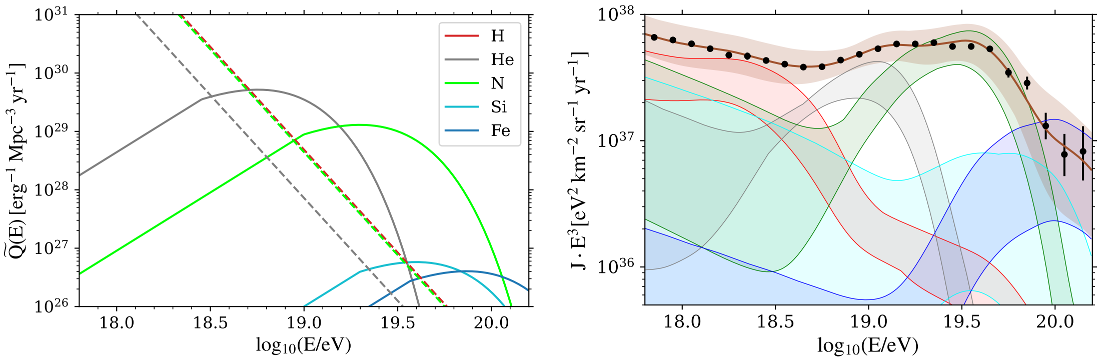

Figure 1: Scenario 2. Left: The generation rate at the extragalactic sources for each representative mass; the two contributions are shown as dashed and solid lines, respectively. Right: The corresponding extragalactic (grouped according to mass number) contributions to the energy spectrum at the top of atmosphere, with their systematic uncertainties.

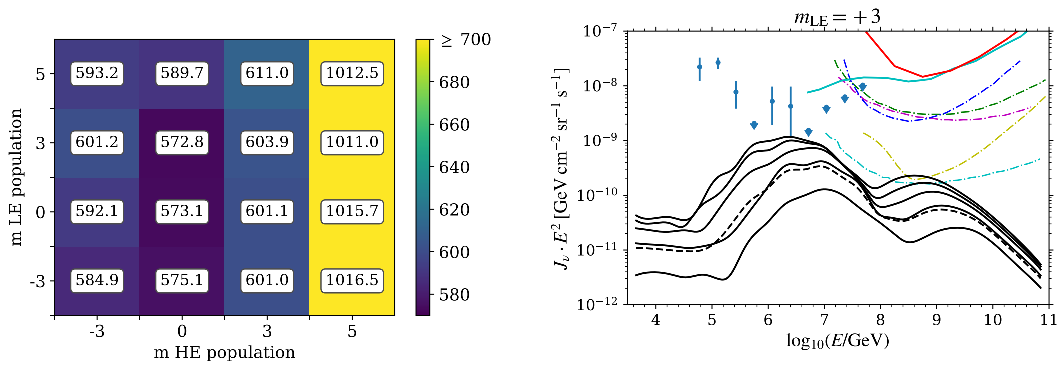

Figure 2: Left: The deviance values obtained for different combinations of source evolution of the two components. Right: The predicted fluxes of neutrinos corresponding to a source evolution with m=3 for the low-energy component. The different black curves represent the fluxes for various choices of maximum redshift z_{max}, from 1 to 5.

Since the values of the minimum deviance are very similar in the two scenarios, a definite conclusion on the presence of a subdominant galactic flux cannot be reached and further investigation of the transition region should be performed. However, our results show that its end is compatible with the data only if it is composed by medium-mass nuclei. The effect of the uncertainties due to measurements and models are also explored. The total effect on the predicted fluxes at the Earth is given by the bands in the right panel of Fig. 1 and is dominated by the uncertainties of the X_{max} measurements. However, it is worth stressing that none of the explored sources of uncertainties spoil our main conclusions.

PoS(TAUP2023)125

Additionally, we examine the impact of the evolution of source emissivity of the two extragalactic populations of sources. We explore various models of evolution parameterized as $(1+z)^m$, with m values of +5, +3, −3, in addition to no-evolution used in the reference case. We find that the source evolution at high redshifts has a minor impact on the LE component and negligible effects on the HE component. We consider different source evolution scenarios for both LE and HE components, resulting in varying total deviance (left panel of Fig. 2). Notably, a strong positive evolution ($m = 5$) for the HE component is disfavored due to excessive flux at ankle energies.

Further constraints can be obtained from the predicted cosmogenic neutrino fluxes: the highest fluxes are expected when assuming a positive source evolution and/or a very high rigidity cutoff for the LE component. Since they are at the level of the sensitivities of future neutrino detectors, next-generation experiments are expected to provide additional constraints on source properties, as shown in the right panel of Fig. 2.

3. Preliminary extensions and outlook

Some ongoing analyses aim to extend the reference fit across the ankle illustrated in the previous section. In Ref. [5], a thicker scan over emissivity evolution parameters is performed and additional constraints on the combination of source evolutions of the two components are set: for example, in presence of a HE component with $m = 4.0$, evolutions with $m \geq 4.6$ are excluded at 90% C.L. for the LE component. Additionally, a preliminary analysis including the effect of the extragalactic magnetic field on the fit results is presented in Ref. [6]. It is shown that, in presence of extragalactic magnetic fields, if the closest sources are far enough, low-energy particles cannot reach the Earth and the energy spectrum appears suppressed at low energy. This is called "magnetic horizon" effect and its inclusion in the model can soften the spectrum of the HE component in some scenarios and will be the object of further investigations in the future.

Other ongoing and future works are expected to provide further interesting results. The inclusion of $X_{\max}$ data from the low-energy extension of Auger, will provide deeper insights into the transition region from galactic to extragalactic cosmic rays. Estimations of mass composition from the Surface Detector data can also be obtained with machine learning techniques, further enhancing these analyses with complementary information [7, 8]. Additionally, mass composition information at the highest energy is expected to improve significantly with the ongoing detector upgrade, AugerPrime [9].

References

[1] The Pierre Auger Coll., *Constraining the sources of ultra-high-energy cosmic rays across and above the ankle with the spectrum and composition data measured at the Pierre Auger Observatory*, *JCAP* **05** (2023) 024.

[2] R. Aloisio et al., *SimProp v2r4: Monte Carlo simulation code for UHECR propagation*, *JCAP* **11** (2017) 009.

[3] T. Pierog et al., *EPOS LHC: Test of collective hadronization with data measured at the CERN Large Hadron Collider*, *Phys. Rev.* **C 92** (2015) 034906.

[4] F. Riehn et al., *Hadronic interaction model* SIBYLL *2.3d and extensive air showers*, *Phys. Rev.* **D 102** (2020) 063002.

[5] C. Petrucci for the Pierre Auger Collaboration, *Constraints on UHECR characteristics from cosmogenic neutrino limits with the measurements of the Pierre Auger Observatory*, PoS(ICRC2023)1520.

[6] J.Gonzalez for the Pierre Auger Collaboration, *Combined fit to the spectrum and composition data measured by the Pierre Auger Observatory including magnetic horizon effects*, PoS(ICRC2023)288.

[7] The Pierre Auger Coll., *Deep-learning based reconstruction of the shower maximum Xmax using the water-Cherenkov detectors of the Pierre Auger Observatory*, *J. Instrum.* **16** (2021) P07019.

[8] The Pierre Auger Coll., *Extraction of the muon signals recorded with the surface detector of the Pierre Auger Observatory using recurrent neural networks*, *J. Instrum.* **16** (2021) P07016.

[9] A. Castellina for the Pierre Auger Collaboration, *AugerPrime: the Pierre Auger Observatory Upgrade*, *EPJ Web Conf.* **210** (2019) 06002.

PoS(TAUP2023)125